Removal of heavy metals from contaminated water using industrial wastes containing calcium and magnesium

Théo Guérin, Nadège Oustrière, David Bulteel, Damien Betrancourt, Alina Ghinet, Sandhya Malladi, Justice Kaleo-Bioh, Amaury Blanc-Brude, Abraham Pappoe, Christophe Waterlot

Removal of heavy metals from contaminated water using industrial wastes containing calcium and magnesium

Théo Guérin[1,2], Nadège Oustrière[1], David Bulteel[1,3], Damien Betrancourt[1,3], Alina Ghinet[2,4,5], Sandhya Malladi[6], Justice G. Kaleo-Bioh[6], Amaury Blanc-Brude[6], Abraham Pappoe[6], Christophe Waterlot[1,*]

[1] Univ. Lille, Institut Mines-Télécom, Univ. Artois, JUNIA, ULR 4515 – LGCgE, Laboratoire de Génie Civil et géo-Environnement, F-59000 Lille, France

[2] JUNIA, Health and Environment, Laboratory of Sustainable Chemistry and Health, F-59000 Lille, France

[3] IMT Lille Douai, Institut Mines-Télécom, Centre for Materials and Processes, F-59000 Lille, France

[4] Univ. Lille, Inserm, CHU Lille, Institut Pasteur de Lille, U1167 - RID-AGE - Facteurs de risque et déterminants moléculaires des maladies liées au vieillissement, F-59000 Lille, France

[5] Faculty of Chemistry, Department of Organic Chemistry, 'Alexandru Ioan Cuza' University of Iasi, Bd. Carol I, nr. 11, 700506, Iasi, Romania

[6] JUNIA, Health & Environment, Team Environment, F-59000 Lille, France

[*] Corresponding author: christophe.waterlot@junia.com

7511 words

Abstract

Two industrial wastes (IW1 and IW2) were investigated as potential sorbents to retain cadmium and lead from contaminated water. The sorption experiments have been conducted through lab-engineered cartridge filtration system in order to get as close as possible to industrial processes. The effectiveness of IW1 and IW2 were compared to that of activated charcoal Norit® (AC), the best-known matrix for its excellent retention capacity. The sorption isotherms of metals on the three solid sorbents (IW1, IW2 and AC) were built, and then mathematically modelled. Free Gibbs energy ($\Delta G°$) of the sorption processes as well as the equilibrium parameter (R_L) have been calculated for each pollutant-sorbent couple. The study revealed that: i) for cadmium sorption, IW2 was much more effective than IW1 and especially than AC (18-fold higher in term of maximal sorption capacity); ii) if IW2 was slightly less effective than AC to retain lead, it can be still considered as an interesting sorbent due to its low cost; iii) the sorption of cadmium was as spontaneous on AC as on IW1, and almost half as much on IW2; iv) regarding lead retention, the sorption on the three sorbents was spontaneous; (v) the retention of cadmium and lead was mainly explained by precipitation since otavite, cerussite and hydrocerussite were identified and characterized by X-ray diffraction of used sorbents. The study showed that the industrial wastes studied stood out as new efficient materials with sorption power equal to or greater than the reference material AC. The prospect of a new generation of industrial wastes with lasting efficiency as contaminated water depollution agents comes at a key moment in the search for new perspectives in the circular economy.

Keywords: sorption; metal; isotherm; water treatment; cartridge filtration technology

1 Introduction

Effects of metal(loid)s on human health and their persistence in environment are a global concern since the 80's. Often referred as heavy metals due to their atomic density, higher than 5 g cm^{-3} (Alloway, 2012), medical diagnosis and reports have proved that some of these metal(loid)s have the potency to cause disabling diseases and human mortality when exposed. For instance, Cd, Pb, Sb and Hg have been designated as four of the ten most dangerous substances to public health (Flora et al., 2012; Bjørklund et al., 2017; Branca et al., 2018; Li et al., 2018). Although they are naturally produced in the environment through various geogenic processes, their rate of production increases due to the anthropogenic sources that span from atmospheric and domestic to commercial activities including agricultural, industrial, pharmaceutical and the release of domestic effluents (He et al., 2005). Consequently, human exposure to metal(loid)s increases at an alarming rate (Tchounwou et al., 2012) and stabilization/removal of these pollutants become a challenge to protect and preserve the environment and health of future generations.

Among the toxic metal(loid)s in wastewater effluents, Cd and Pb were cited as the main ones since they are respectively classified as CARC2/MUTA3/REPRO3 and CARC1/REPRO1/REPRO3) in the Regulatory European Classification of CMR chemicals. Considering the serious health consequences (Akpor et al., 2014), removal of these two metals from contaminated water has been extensively studied through various techniques and devices, including chemical precipitation, complexation, ion exchange, reverse osmosis and sorption. Chemical and physical sorption have been extensively studied considering organic and metal(loid)s pollutants and various sorbents like graphene, activated carbons, carbon nanotubes, magnetic sorbents, alumina, zeolites, kaolin, phosphate rocks, Mn-oxyhydroxyde, mesoporous silica, clays, chitosan, modified or not modified agricultural wastes, bio-sorbent, biomass-based materials and nanostructured materials (Sari et al., 2008; Karnib et al., 2014; Abdel-Raouf and Abdul-Raheim, 2017; Asuquo et al., 2017; Bisht et al., 2017; Feng et al., 2017; Burakov et al.,

2018; Tariq et al. 2018; Joseph et al., 2019; Ani et al., 2020; Boni et al., 2020) or mixture of mineral and organic materials (Fu et al., 2020). Among mineral materials, oxides nanomaterials have been extensively studied in the wastewater treatment with the aim to sorb organic pollutants and/or metal(loid)s (Xu et al., 2012; Davé and Chopda., 2014; Lu et al., 2016; Atkovska et al., 2018; Santhosh et al., 2019; Yaqoob et al., 2020). In contrast, and according to our knowledge, only few studies reported the removal of metal(loid)s from water using non-nanomaterials oxides (*e.g.* goethite, birnessite, magnetite; Fe-Al binary oxides; Hong et al., 2017; El Haouti et al., 2018; Ugwu and Igbokwe, 2019). Some of these oxides (Fe, Al and Mn) originated from industrial wastes while others resulted from water treatment residuals (Jacukowicz-Sobala et al., 2015; Ghorpade and Ahammed, 2018; Wolowiec et al., 2019).

Among industrial wastes, the production of fertilisers (*e.g.* calcium or magnesium carbonate) generates a large quantity of by-products rich in calcium and magnesium. Valorising these industrial wastes as metal(loid) sorbents would fulfil the EU policy that encourage the re-use of industrial by-products. To date, industrial wastes from the process used to obtain pure calcium and magnesium carbonates and oxides have never been studied as sorbent of metal(loid)s from contaminated water. Towards this direction, the current study focused on the removal of two carcinogenic, mutagen and reprotoxic pollutants (Cd and Pb) using two industrial wastes (low-cost products) and activated carbon as reference.

2 Materials and Methods

2.1 Metal pollutants

The current study focused on artificial contaminated water by Cd and Pb. Cadmium sulfate ($CdSO_4$) and lead acetate ($(CH_3CO_2)_2Pb$) were diluted to obtain metal solutions (10, 20, 40, 60, 80, 100, 150, 200, 250, 350, 500, 1 000, 2 000, 2 500, 5 000, 10 000, 15 000, 20 000, 25 000 mg L^{-1}) in ultra-pure water. Knowing that 25 mL of artificial contaminated water were eluted

on the lab-made cartridge (section 2.3), the amount of Cd or Pb ranged from 0.25 up to 625 mg. The last mass is quite similar to the mass of cadmium removed from aqueous solution using poly(acrylic acid) stabilized amorphous calcium carbonate nanoparticles (Cai et al., 2010).

2.2 Sorbents

Activated Carbon (AC; Norit SA-2, Acros organics®) without any modification was chosen as reference since it is the most used sorbent, known for its very high adsorption capacity. Nevertheless, it is very expensive (Feng et al., 2017). The properties of this material are as follows: iodine number: 850; specific surface area: 950 m^2 g^{-1}; apparent density: 460 kg m^{-3}; particle size D_{10}: 3 µm; particle size D_{50}: 20 µm; particle size D_{90}: 140 µm; ash content: 9%.

Two industrial wastes (IW1 and IW2), defined as by-products by the Scora company (Caffiers, France) were evaluated in the retention of the studied metal pollutants (Cd and Pb). They were dried at 105 °C before crushing and sieving with a mesh size of less than 315 µm. The metal concentrations in these industrial wastes were assessed after their *aqua-regia* digestion by flame atomic absorption spectrometry (FAAS; AA-6800 Shimadzu, Tokyo, Japan; Waterlot and Douay, 2009; Savio et al., 2010; Waterlot and Hechelski, 2019). The results were summarised in Table 1. The particle-size distribution of both industrial wastes was measured using a particle-size analyser (Mastersizer 3000; Malvern Panalytical; United Kingdom).

X-ray diffraction (XRD) data measurements on the samples before and after pollutants elution dried at 110 °C for 2 h were performed by using a diffractometer BRUKER D8 with an anticathode in cobalt ($\lambda K\alpha_1$ = 1.74 Å) equipped with a LynxEye detector. The X-ray patterns were acquired in the 2θ (10–80°) with a step size of 0.02° and 89.5 s per step (Kleib et al., 2018).

2.3 Sorption experiments

The columns used in the current study were from Teledyne Technologies Inc. (Redisep Rf column), measuring 8 cm in length and having a diameter of 1.5 cm. They were filled with

200 mg of compacted cotton on top of which, 1 g of industrial waste were added. The surface of each sorbent powder layer was then flattened in order to obtain a homogeneous surface. The artificial contaminated water (25 mL, $n = 3$) was then eluted on the lab-made cartridge. The filtered contaminated solutions were then kept in amber glass pillboxes and stored at 4 °C prior to analysis. Note that all experiments were conducted under normal temperature and pressure conditions (20 °C; 1 atm).

2.4 Sorbate analysis

At the end of the sorption experiments, the concentrations of Cd and Pb in solutions were measured by FAAS without any sample preparation, except dilution if necessary. Specifications on analyses were detailed in Waterlot et al. (2011). Limits of detection (LD) in water were 2.1 µg L^{-1} and 41 µg L^{-1} for Cd and Pb, respectively (Waterlot and Hechelski, 2019).

2.5 Data analysis

The sorption isotherms were investigated using two equilibrium models, which are namely the Freundlich and Langmuir models. The Freundlich isotherm model was used as its linear equation (eq. 1).

$$\ln q_e = \ln K_f + 1/n \ln C_e, \quad (1)$$

where q_e is the amount of pollutant adsorbed per g of sorbent (mg g^{-1}), C_e is the equilibrium concentration of the adsorbate (mg L^{-1}), K_f and n are both the Freundlich constants, the first represents the relative adsorption capacity of the sorbent (mg$^{1-(1/n)}$ $L^{1/n}$ g^{-1}) and the second gives information about adsorption intensity (dimensionless).

The Langmuir isotherm was used under its linear form as well (eq. 2).

$$1/q_e = 1/ C_e b q_m + 1/q_m, \quad (2)$$

where q_e is the amount of pollutant adsorbed per g of sorbent (mg g^{-1}), C_e represents the equilibrium concentration of the adsorbate material (mg L^{-1}), q_m is the maximum adsorption

125 capacity (mg g^{-1}) and b is a constant associated to the free energy of adsorption (L mg^{-1}). The
126 latter is very interesting because it is related to the Gibbs free energy (eq. 3) (Djelloul 2014).

127 $$\text{Ln } (1/b) = \Delta G°/RT, \qquad (3)$$

128 where $\Delta G°$ is the Gibbs free energy of the sorption reaction (J mol^{-1}), *b* is a constant associated
129 to the free energy of adsorption (L mol^{-1}), T is the temperature (K) and R the universal gas
130 constant (J mol^{-1} K^{-1}). This Gibbs free energy is expressed by the equation (4).

131 $$\Delta G° = - RT \ln b, \qquad (4)$$

132 The Hall parameter (or equilibrium parameter) (Hamdaoui and Naffrechoux, 2007) was
133 calculated according to the following equation 5.

134 $$R_L = 1/(1 + b*C_0) \qquad (5)$$

135 where C_0 is the initial concentration of the adsorbate in solution (mg L^{-1}) and *b* is a constant
136 associated to the free energy of adsorption (L mg^{-1}).

137 ***2.6 Statistical analysis***

138 Influence of the three solid sorbents (IW1, IW2 and AC) on Cd and Pb concentrations
139 measured in the filtered solutions were tested using a one-way analysis of variance (ANOVA)
140 at all exposure concentrations. Normality and homoscedasticity of residuals were met for all
141 tests. When significant differences occurred between treatments, multiple comparisons of mean
142 values were made using post-hoc Tukey HSD tests. Differences were considered statistically
143 significant at $p<0.05$. Changes in Cd and Pb concentration in the filtered solutions depending
144 on the initial exposure concentrations, the solid sorbents (IW1, IW2 and AC), and their
145 interaction were analysed for both contaminants (Cd and Pb) using an ANCOVA followed by
146 post-hoc Tukey analysis to test the different ANCOVA models using the R package
147 "multcomp". All statistical analyses were performed using R software (version 3.0.3,
148 Foundation for Statistical computing, Vienna, Austria).
149

3 Results and discussion

3.1 Sorption capacity of Activated Carbon (AC)

Sorption isotherms of Cd and Pb on activated carbon were plotted in Figures 1A and 1D, respectively. Opposingly to Pb (Fig. 1C), a non-linear Freundlich isotherm was obtained for Cd by plotting q_e versus C_e values (Fig. 1A). The results showed that Pb was better adsorbed than Cd. The equilibrium data were analysed using the linearized form of Freundlich equation (eq. 1) by plotting $\ln q_e$ versus $\ln C_e$ (Fig. 1B & 1E). The coefficients of determination were higher for Pb (0.999) than for Cd (0.985) showing a good linearity for both metals. The Freundlich constants $K_{f\text{-}Cd}$ and $K_{f\text{-}Pb}$ were 0.210 $mg^{1-(1/n)}\ L^{1/n}\ g^{-1}$ and 0.0990 $mg^{1-(1/n)}\ L^{1/n}\ g^{-1}$, and constants n_{Cd} and n_{Pb} were 1.25 and 1.00, respectively. These results mean that the relative sorption of Cd when the equilibrium equals 1 mg L^{-1} is higher than that of Pb. On the other hand, the sorption intensity of Cd is 25% higher than that of Pb. Although these trends correlated well with the conclusion in Asuquo et al. (2017), the Freundlich constants were somewhat at odds with those found by these authors ($K_{f\text{-}Cd}$ = 6.99; $K_{f\text{-}Pb}$ = 6.53; n_{Cd} =4.00; n_{Pb} = 4.85) probably due to the BET surface area, 4273 $m^2\ g^{-1}$ in Asuquo et al. (2017) and 950 $m^2\ g^{-1}$ in the current study. In the same way, the Freundlich constants obtained by Gaya et al. (2015) were below from this study ($K_{f\text{-}Cd}$ = 0.02; $K_{f\text{-}Pb}$ = 0.02; n_{Cd} = 1.00; n_{Pb} = 1.00) using a regular activated carbon due to its very low BET surface area (< 5.41 $m^2\ g^{-1}$).

Asuquo et al. (2017) demonstrated that the Freundlich isotherm is less suitable for the description of Cd-sorption than the Langmuir isotherm. It is the most widely used model to describe the sorption of a solute from contaminated water since the basic theory considers that sorption takes place at specific homogeneous sites within the sorbent. The Langmuir isotherms of Cd and Pb were plotted in Figures 1C and 1F. As shown in these two graphs, very good linear curves were obtained, the coefficients of determination being 0.995 for Cd and > 0.999 for Pb. The values of maximum adsorption capacity using the Langmuir equation were 247 mg

175 Cd g^{-1} and 3488 mg Pb g^{-1}. These values seem somewhat at odds with those reported in literature
176 (Minceva et al., 2008; Asuquo et al., 2017; Okeola et al., 2017; Joseph et al., 2019).
177 Nevertheless, the study of Karnib et al. (2014) showed maximum adsorption around 178 mg
178 Cd g^{-1} on AC and up to 1000 mg Pb g^{-1} using treated NaOH-AC (Gaya et al., 2015). Anyway,
179 Pb ions had a greater accessibility to the AC surface than Cd. This experimental result correlated
180 well with the theory on solid surfaces since metal(loid)s of higher electronegativity and shorter
181 hydrated ionic radius should adsorb more readily (Minceva et al., 2008).

182 ***3.2 Sorption capacity of Industrial Waste (IW)***

183 *3.2.1 Characterization*

184 The particle size distribution was D_{10}: 29 µm; D_{50}: 153 µm; D_{90}: 344 µm, for IW1 and D_{10}:
185 7 µm; D_{50}: 103 µm; D_{90}: 753 µm for IW2. The metal concentrations were reported in Table 1.
186 The great difference between the two sorbents is the percentage of calcium and magnesium,
187 respectively 3.8-fold lower and higher in IW2 than in IW1. It is worth mentioning that the
188 concentrations of K, Al, Fe, Mn, Pb, Zn and As are the highest in IW1. The XRD analysis
189 revealed the presence of two crystalline species in IW1 and IW2 (Figures 2A, 2B, respectively).
190 Calcite ($CaCO_3$) and quartz (SiO_2) were the two main crystalline species in IW1 whereas
191 hydromagnesite ($Mg_5(CO_3)_4(OH)_2$, $4H_2O$) and calcite were identified in IW2.

192 *3.2.2 Removal capacity of Cd and Pb by IW1*

193 As shown in Figure 3 (3A, 3B, 3D and 3E), the Freundlich models (non-linearized and
194 linearized) were not appropriate to explain the sorption processes of Cd and Pb. It is well
195 accepted that the Freundlich model assumes heterogeneous adsorption surface and active sites
196 with different energy. For both metals, this sorption process can be successfully applied for
197 sorbed metal concentrations below 90 mg Cd g^{-1} and 125 mg Pb g^{-1}. In contrast, the Langmuir
198 sorption isotherm has been successfully applied to Cd and Pb sorption processes (Fig. 3C &
199 3F). Excellent coefficients of determination were obtained for both metals ($R^2 > 0.999$), which

means that Langmuir was the most suitable model to describe the sorption process of Cd and Pb on IW1. Similar trend has been already mentioned with metal oxides sorbents (Trivedi et al., 2001; Kumar et al., 2014; Guo et al., 2018). The values of maximum adsorption capacity using the Langmuir equation were 311 mg Cd g^{-1} and 1575 mg Pb g^{-1}. These results correlated well with those described in the literature since the sorption of both metals on nano-metal (Zn, Ti, Al, Mn, Fe) oxides ranged from 29 to 625 mg Cd g^{-1} and reached up to 780-1128 mg Pb g^{-1}, depending on the sorbent, the temperature, the duration contact and the pH (Kumar et al., 2014; Guo et al., 2018; Liu et al., 2018).

The solid sorbents IW1-Cd and IW1-Pb were analysed by XRD after the filtration of Cd and Pb contaminated water on IW1. The X-ray diffractogram (Figure 4) revealed the presence of otavite ($CdCO_3$) and hydrocerussite ($Pb_3(CO_3)_2(OH)_2$). The retention of Cd and Pb from contaminated water by $CaCO_3$ or $CaCO_3$-based nanoadsorbents was well documented, as well as their respective mechanisms (McBride, 1980; Rangel-Porras et al., 2010; Mlayah and Jellali, 2015; Ponomarev et al., 2019; Wang et al., 2020). Depending on pH, precipitates like otavite, cerussite ($PbCO_3$) or hydrocerussite were identified and mechanisms related to precipitation, complexation and chemisorption were highlighted. The difference between Cd^{2+} and Pb^{2+} is their ionic radius, explaining that at low concentration of Cd^{2+}, substitution of Ca^{2+} in accessible surface sites occurred (the ionic radius of Cd^{2+} being similar to Ca^{2+}). Cai et al. (2020) demonstrated that $CdCO_3$ was not simply the result of the reaction between Cd^{2+} and CO_3^{2-} but the result of two consecutive mechanisms, the first step being an adsorption onto the amorphous calcite surface and the second one, a precipitation from $CaCO_3$ to $CdCO_3$. At high levels of Cd and Pb in water, the highest affinity of calcite for Pb was demonstrated (Rangel-Porras et al., 2010) and, depending on solids and the initial concentration of contaminated samples, removal capacities of Cd and Pb were up to 821 mg g^{-1} and 1350 mg g^{-1}, respectively (Mlayah and Jellali, 2015; Wang et al., 2020).

It is worth mentioning that the disadvantage of using IW1 is its high concentration of Al, Zn and As (Table 1). In view of the sorption capacity of this sorbent, the use of another solid sorbent with lowest metal concentrations would be preferable for a safety utilization.

3.2.3 Removal capacity of Cd and Pb by IW2

The Freundlich and Langmuir isotherms of Cd and Pb on the second industrial waste (IW2) were summarized in Figure 5. Non-linearized and linearized Freundlich isotherms of Cd (Fig. 5A & 5B) and Pb (Fig. 5D & 5E) using IW2 were better than those obtained with IW1 since good determination coefficients were obtained for both metals ($R^2 > 0.999$). The Freundlich constants $K_{f\text{-}Cd}$ and $K_{f\text{-}Pb}$ were 0.026 $mg^{1-(1/n)}$ $L^{1/n}$ g^{-1} and 0.025 $mg^{1-(1/n)}$ $L^{1/n}$ g^{-1}, and constants n_{Cd} and n_{Pb} were 1.01 and 0.99, respectively. Therefore, the relative sorptions of Cd and Pb when the equilibrium equals 1 mg L^{-1} are the same. The equilibrium data analysed using the linearized form of Langmuir equation (eq. 2) was obtained by plotting $1/q_e$ versus $1/C_e$ (Fig. 5C & 5F). The determination coefficients were also higher than 0.999 for Cd and Pb, meaning that Freundlich and Langmuir isotherms were suitable for the description of experimental data. The values of the maximum adsorption capacity using the Langmuir equation were 4569 mg Cd g^{-1} and 2638 mg Pb g^{-1}. These values are significantly higher than those reported with IW1. Analysis of IW2 reveals the presence of Ca (5.8%; Table 1) and Mg (21%). In fact, both of these metals exist as $CaCO_3$ (14.5%) and $Mg_5(CO_3)_4(OH)_2.4H_2O$ (74%) from the crude material (Figure 2B). The XRD analyses of IW2 after the filtration of Cd or Pb from contaminated water (named IW2-Cd and IW2-Pb, respectively) showed the presence of otavite in IW2-Cd and cerussite and hydrocerussite in IW2-Pb (Figure 6). Affinities of Cd and Pb for magnesium oxides are also well known and are similar to calcium oxides. Another mechanism was demonstrated using flowerlike MgO nanostructures to explain the high capacity (1980 mg Cd g^{-1} and 1500 mg Pb g^{-1}) of magnesium oxides (Cao et al., 2012). The authors explained these results by a solid-liquid interfacial cation exchange between magnesium and both metals

studied (Cd and Pb) as adsorption mechanism that depends on the ability of hydrated-metal to lose their outer hydration sphere to give hydroxyl-metal complexes. Pehlivan et al. (2009) reported the effectiveness of natural Turkish dolomite ($CaMg(CO_3)_2$) for removing Pb from aqueous solution. The authors stated that metal adsorption on dolomite surfaces has been described in terms of two mechanisms that are cation exchange in the interlayer and specific adsorption resulting from surface complexation at low concentration, as it was observed with calcite sorbent. In contrast, precipitation mechanism occurred at high concentration following two steps; first, Pb ions adsorb onto calcite and then move into Ca sites, despite the large ionic radius of Pb^{2+} relative to Ca^{2+} (Sturchio et al., 1997).

3.3 Efficiency of the solid sorbents

If we consider the overall concentration range, 10-25000 mg L^{-1}, Cd and Pb retention in sorbents depended on both the sorbents type and the initial concentration in solution (Table 2, 3, $p<10^{-4}$) but interactions between both factors were not significant ($p>0.05$). Thus, Cd and Pb retentions were significantly higher in the AC ($p<0.001$) compared to both oxides, but they were not significantly different between IW1 and IW2 ($p>0.05$). Only for an initial concentration higher than 20000 mg L^{-1}, Cd retention in IW2 and AC were not statistically different (Supplementary material 1). For initial concentration in solution higher than 2000 mg Cd L^{-1} or 5000 mg Pb L^{-1}, Cd and Pb retentions were significantly higher in IW2 than in IW1. From a practical point of view, these results mean that AC was superior to IW1 and IW2 for Pb and Cd when their concentrations in solution were below 2000 mg L^{-1}. However, the choice of the sorbent depends on the strategy used in the water treatment process. Indeed, IW2 is cheaper than AC and its sorption capacity the highest. The Langmuir parameter q_m of the three sorbents for Cd and Pb must be compared, as it is closely related to sorption efficiency. Depending on the sorbent, q_m may be ordered according to their efficiency to sorb Cd as: IW2 > IW1 > AC (4569 mg Cd g^{-1}, 311 mg Cd g^{-1} and 247 mg Cd g^{-1}, respectively). For Pb sorption, this order

was AC > IW2 > IW1 (3488 mg Pb g^{-1}, 2638 mg Pb g^{-1} and 1575 mg Pb g^{-1}). In view of these results, IW2 appeared as the most effective sorbent for the Cd retention, 15-fold higher than IW1 and 18-fold higher than AC used as reference. However, although IW2 presented a better Pb sorption capacity compared to IW1 (1.7-fold higher), it was less effective than AC (1.3-fold smaller).

The most recent literature review related to the removal of metals using adsorbents adsorption of metals reported a classification of these materials. Thus, it is well accepted that they can be classified according to carbon based materials (activated carbon, activated carbon cloth, activated carbon fibre), nanomaterials (nanoparticules, nanotubes, nanorods, nanowires), composite and nanocomposite adsorbents, miscellaneous adsorbents and low-cost adsorbents. Low-cost materials are divided into three subclasses depending on their origin: agriculture solid waste and industrial by-products (metal(hydr)oxides, waste slrry, fly ash, red mud, bio-solids), natural materials (clays, zeolites, silica, alumina, kaolinite, bentonite, montmorillonite, chitosan and (hydr)oxides) and bio-sorbents (biopolymers, peat and biomass). According to the dataset from several reviews (Renu et al., 2017; Joseph et al., 2019; Wilowiec et al., 2019; Gupta et al., 2021; Qasem et al., 2021; Zaimee et al., 2021), the most relevant adsorbents for Cd are modified chitosan (q_m = 248 mg g^{-1}), orange peel (q_m = 248 mg g^{-1}), razor clam shells (q_m = 501 mg g^{-1}), zeolite (q_m = 649 mg g^{-1}), graphene oxides (q_m up to 793 mg g^{-1}), metal oxides (q_m up to 1500 mg g^{-1}). For Pb, the authors reported excellent retention with zeolite (q_m = 210 mg g^{-1}), razor clam shells (q_m = 657 mg g^{-1}), graphene oxides (q_m up to 1000 mg g^{-1}), oyster shells (q_m = 1591 mg g^{-1}), nanocomposites (q_m = 1167 mg g^{-1}) and metal oxides (q_m up to 3900 mg g^{-1}). This means that the two industrial wastes (IW1 and IW2) studied are in the top ranking of adsorbents according to their Cd and Pb retention capacity and IW2 is the best-known Cd-adsorbent described in the literature.

3.4 Thermodynamic characteristics of the solid sorbents

To go further from a thermodynamic point of view, the Gibbs free energy (ΔG°) of the sorption processes of Cd and Pb on AC, IW1 and IW2 has been calculated from eq. 4 using the Langmuir parameter *b* (Djelloul 2014). For Cd sorption, the numerical values of ΔG° were negative and followed the order AC < IW1 < IW2 (-14.91 KJ mol^{-1}, -14.35 KJ mol^{-1} and -7.81 KJ mol^{-1}, respectively). In this regard, the sorption phenomenon of Cd onto the three sorbents were found to be exergonic. However, it is important to mention that the spontaneous sorption processes of Cd on AC and IW1 were similar and 1.9-fold higher than IW2. For Pb sorption, values of ΔG° are also negative and can be ordered as follows: IW1 < IW2 < AC (-11.890 KJ mol^{-1}, -10.635 KJ mol^{-1} and -9.954 KJ mol^{-1}, respectively). In this case, we can considerer similar values of free energy meaning that Pb sorption on the three sorbents studied proceed spontaneously forward the formation of products in equivalent amounts.

The Hall parameter (R_L, also called equilibrium parameter) was assessed from the Langmuir parameter *b* according to the equation 5 (Hamdaoui and Naffrechoux, 2007). Depending on the sign of this parameter, the sorption is defined as irreversible ($R_L = 0$), favourable ($0 < R_L < 1$), linear ($R_L = 1$) or unfavourable ($R_L > 1$). Similarities in the R_L values were highlighted for Cd with AC and IW1 (Figure 7A). In both cases, R_L values drastically decreased from 0.80 to 0.11, and then below 0.1 from 2500 to 25 000 mg L^{-1}. This result indicated that the sorption is favourable in the range of the Cd concentration studied. In addition, the higher the initial concentration, the more favourable the sorption is, even tending towards an irreversible phenomenon. To a lesser extent, the R_L values also decreased with IW2 when the initial Cd concentration of the solution increased. Indeed, it ranged from 0.98 to 0.15, demonstrating a favourable sorption. Note that the lowest R_L values obtained with AC and IW1 correlated well with the lowest values of the Gibbs energy, which corroborates with the fact that the Cd sorption on AC and IW1 was more spontaneous and less reversible than on IW2. For Pb, values and evolution of the R_L obtained with AC, IW1 and IW2 are shown in Figure 7B. For these three

solid sorbents, all parameters dropped similarly when Pb concentrations increased. However, values for this parameter were quite different, ranging from 0.98 to 0.12 for AC, from 0.95 to 0.059 for IW1 and from 0.97 to 0.095 for IW2. In all cases, these values confirmed the favourable nature of the Pb sorption on the sorbents studied and correlated well with the order of the sequence AC > IW2 > IW1 established regarding the free Gibbs energy.

4 Conclusions

Two industrial by-products (IW1 and IW2) were evaluated as sorbent for the retention of Pb and Cd from artificially contaminated water. In order to be able to conclude on the effectiveness of IW1 and IW2 as sorbent for Cd and Pb, all experiments were carried out in parallel on activated charcoal Norit® (AC), the best-known matrix for its excellent retention capacity. The aqueous solutions of Cd and Pb (from 10 to 25 000 mg L^{-1}) were eluted on lab-engineered cartridges filled with the selected solid sorbents in order to be close to industrial practices.

Sorption isotherms were constructed and investigated according to the mathematical models of Freundlich and Langmuir. In addition, free Gibbs energy of the sorption processes ($\Delta G°$) as well as the equilibrium parameter (R_L) have been calculated for each pollutant-sorbent couple and were compared. All these data allowed to conclude that for Cd sorption, IW2 was much more effective than IW1 (15-fold higher) and AC (18-fold higher). The sorption of Pb was more important on AC than on IW2 (1.3-fold higher) which retains itself 1.9-fold more Pb than IW1. The X-ray diffraction indicated the presence of otavite, cerussite and hydrocerussite in the solid sorbents suggesting that sorption of Cd and Pb was based on precipitation mechanism. Finally, the calculations of $\Delta G°$ and R_L have revealed that the sorption of Cd is as spontaneous on AC as on IW1, and almost half as much on IW2. Regarding Pb retention, the sorption on the three sorbents is spontaneous and no significant deviation was observed. Further experiments are necessary to check the sorption capacity of other divalent cations by these two industrial wastes.

Acknowledgments

The authors thank the Région Hauts-de-France and JUNIA for financial support (FEDER funding) of this work and technical help and facilities. The authors also acknowledge the Scora company, Caffiers, France, for providing calcium and magnesium oxides-based industrial wastes investigated in the current study.

Declaration of competing interest

The authors declare that they have no known competing financial interests or personal relationships that could have appeared to influence the work reported in this paper.

References

Abdel-Raouf, M.S., Abdul-Raheim, A.R.M., 2017. Removal of heavy metals from industrial waste water by biomass-based materials: A review. Journal of Pollution Effects & Control 5, 180–193. https://doi.org/10.4172/2375-4397.1000180.

Ani, J.U., Akpomie, K.G., Okoro, U.C., Aneke, L.E., Onukwulli, O.D., Ujam, O.T., 2020. Potentials of activated carbon produced from biomass materials for sequestration of dyes, heavy metals, and crude oil components from aqueous environment. Appl. Water Sci. 10, 69–80. https://doi.org/10.1007/s13201-020-1149-8.

Asuquo, E., Martin, A., Nzerem, P., Siperstein, F., Fan X., 2017. Adsorption of Cd(II) and Pb(II) ions from aqueous solutions using mesoporous activated adsorbent: Equilibrium, kinetics and characterization studies. J. Environ. Chem. Eng. 5, 679–698. https://doi.org/10.1016/j.jece.2016.12.043.

Alloway, B.J., 2012. Heavy metals in soil: Trace metals and metalloids in soils and their boavailability, third ed. Environmental Pollution, Springer Netherlands.

374 Apkor, O.B., Ohiobor, G.O., Olaolu, T.D., 2014. Heavy metal pollutants in wastewater
375 effluents: Sources, effects and remediation. Advances in Bioscience and Bioengineering 2, 37–
376 43. https://doi.org/10.11648/j.abb.20140204.11.
377 Atkovska, K., Lisichkov, K., Ruseka, G., Domitrov, A.T., Grozdanov, A., 2018. Removal of
378 heavy metal ions from wastewater using conventional and nanosorbents: A review. J. Chem.
379 Technol. Metallurgy 53, 202–219. https://doi.org/10.1007/978-3-319-71279-633.
380 Bjørklund, G., Dabar, M., Mutter, J., Aaseth, J., 2017. The toxicology of mercury: Current
381 research and emerging trends. Environ. Res. 159, 545–554.
382 htpps://doi.org/10.1016/j.envres.2017.08.051.
383 Bisth, R., Agarwal, M., Singh, K., 2017. Heavy metal removal from wastewater using various
384 adsorbents: a review. J. Water Reuse Desalin. 7, 387–419.
385 https://doi.org/10.2166/wrd.2016.104.
386 Boni, M.R., Chiavola, A., Marzeddu, S., 2020. Remediation of lead-contaminated water by
387 virgin coniferous wood biochar adsorbent: batch and column application. Water Air Soil Pollut.
388 231, 171–187. htpps://doi.org/10.1007/s11270-020-04496-z.
389 Branca, J.J.V., Morucci, G., Pacini, A., 2018. Cadmium-induced neurotoxicity: still much ado.
390 Neural Regen. Res. 13, 1878–1882. https://doi.org/10.4103/1673-5374.239434.
391 Burakov, A.E., Galunin, E.V., Burakova, I.V., Kucherova, A.E., Agarwal, S., Tkachev, A.G.,
392 Gupta, V.K., 2018. Adsorption of heavy metals on conventional and nanostructured materials
393 for wastewater treatment purposes: A review. Ecotoxicol. Environ. Safe. 148, 702–712.
394 https://doi.org/10.1016/j.ecoenv.2017.11.034.
395 Cai, G.-B., Zhao, G.-X., wang, X.-K., Yu, S.-H., 2010. Synthesis of polyacrylic acid stabilized
396 amorphous calcium carbonate nanoparticles and their application for removal of toxic heavy
397 metals ions in water. J. Phys. Chem.114, 12948–12954. https://doi.org/10.1021/jp103464p.

398 Cao, C-Y., Qu, J., Wei, F., Liu, H., Song W-G., 2012. Superb Adsorption Capacity and
399 Mechanism of Flowerlike Magnesium Oxide Nanostructures for Lead and Cadmium Ions. ACS
400 Appl. Mater. Interfaces 4, 4283–4287. https://doi.org/10.1021/am300972z.
401 Dave, P.N., Chopda, L.V., 2014. Application of iron oxide nanomaterials for the removal of
402 heavy metals. Journal of Nanotechnology Article ID 398569, 1–14.
403 https://doi.org/10.1155/2014/398569.
404 Djelloul, K., 2014. Expérimentation, modélisation et optimisation de l'adsorption des effluents
405 textiles. Thesis, University Mohamed Khider De Briska, 116 pp.
406 El Haouti, R., Anfar, Z., Et-Taaleb, S., Benafqir, M., Lhanafi, S., El Alem, N., 2018. Removal
407 of heavy metals and organic pollutants by a sand rich in iron oxide. Euro-Mediterr. J. Environ.
408 Integr. 3, 17–34. https://doi.org/10.1007/s41207-018-0058-9.
409 Feng,Y., Liu, Y., Xue, L., Sun, H., Guo, Z., Zhang, Y., Yang, L., 2017. Carboxylic acid
410 functionalized sesame straw: a sustainable cost-effective bio adsorbent with superior dye
411 adsorption capacity. Biores. Technol. 238, 675–683.
412 https://doi.org/10.1016/j.biortech.2017.04.066.
413 Flora, G., Gupta, D., Tiwari, A., 2012. Toxicity of lead: A review with recent updates. Toxicol.
414 5, 47–58. https://doi.org/10.2478/v10102-012-0009-2.
415 Fu, C., Zhang, H., Xia, M., Lei W., Wang, F., 2020. The single/co-adsorption characteristics
416 and microscopic adsorption mechanism of biochar-montmorillonite composite adsorbent for
417 pharmaceutical emerging organic contaminant atenolol and lead ions. Ecotoxicol. Environ.
418 Safe. 187, 109763. https://doi.org/10.1016/j.ecoenv.2019.109763.
419 Gaya, U.I., Otene, E., Abdullah, A.H., 2015. Adsorption of aqueous Cd(II) and Pb(II) on
420 activated carbon nanopores prepared by chemical activation of doum palm shell. SpringerPlus
421 4, 458–476. https://doi.org/10.1186/s40064-015-1256-4.

422 Ghorpade, A., Ahammed, M.M., 2018. Water treatment sludge for removal of heavy metals
423 from electroplating wastewater. Environ. Eng. Res. 23, 92–98.
424 https://doi.org/10.4491/eer.2017.065.
425 Guo, T., Bilun, C., Li, B., Zhao, Z., Yu, H., Sun, H., Ge, X., Xing, R., Zhang, B., 2018. Efficient
426 removal of aqueous Pb(II) using partially reduced graphene oxide-Fe_3O_4. Adsorp. Sci. Technol.
427 36, 1031–1048. https://doi.org/10.1177/0263617417744402.
428 Gupta, K., Joshi, P., Gusain, R., Khatri, O.P. 2021. Recent advance in adsorptive removal of
429 heavy metal and metalloid ions by metal oxide-based nanomaterials. Coord. Chem. Rev. 445,
430 214100. https://doi.org/10.1016/j.ccr.2021.214100.
431 Hamdaoui, O., Naffrechoux, E., 2007. Modeling of adsorption isotherms of phenol and
432 chlorophenols onto granular activated carbon Part I. Two-parameter models and equations
433 allowing determination of thermodynamic parameters. J. Hazard. Mater. 147, 381–394.
434 https://doi.org/10.1016/j.jhazmat.2007.01.021.
435 He, Z.L., Yang, X.E., Stoffela, P.J., 2005. Trace elements in agrosystems and impacts on the
436 environment. J. Trace Elem. Med. Biol. 19, 125–140.
437 https://doi.org/10.1016/j.jtemb.2005.02.010.
438 Hong, H.J., Yang J.W., Yang, J.S., Jeong, H.S., 2017. Highly enhanced heavy metal adsorption
439 performance of iron oxide (Fe-oxide) upon incorporation of aluminium. Mater. Trans. 58, 71–
440 75. https://doi.org/10.2320/matertrans.M2016277.
441 Jacukowicz-Sobala, I., Ociński, D., Kociołek-Balawejder, E., 2015. Iron and aluminium oxides
442 containing industrial wastes as adsorbents of heavy metals: Application possibilities and
443 limitations. Waste Manag. Res. 33, 612–629. https://doi.org/10.1177/0734242X15584841.
444 Joseph, L., Jun, B.M., Flora, J.R.V., Park, C.M., Yoon, Y. 2019. Removal of heavy metals from
445 water sources in the developing world using low-cost materials: A review. Chemosphere 229,
446 142–159. https://doi.org/10.1016/j.chemosphere.2019.04.198.

447 Kumar, R., Chawla, J. 2014. Removal of cadmium ion from water/wastewater by nano-metal
448 oxides: A review. Water Qual. Expo. Health 5, 215–226. https://doi.org/10.1007/s12403-013-
449 0100-8.
450 Liu, Z., Zhong, X., Wang, Y., Ding, Z., Wang, C., Wang, G., Liao, S., 2018. An Efficient
451 Adsorption of Manganese Oxides/Activated Carbon Composite for Lead(II) Ions from Aqueous
452 Solution. Arab. J. Sci. Eng. 43, 2155–2165. https://doi.org/10.1007/s13369-017-2514-2.
453 Lu, H., Wang, J., Stoller, M., Wang, T., Bao, Y., Hao, H., 2016. An overview of nanomaterials
454 for water and wastewater treatment. Advances in Materials Science and Engineering Article ID
455 4964828, 1–10. https://doi.org/10.1155/2016/4964828.
456 Karnib, M., Kabbani, A., Holail H., Olama Z., 2014. Heavy metals removal using activated
457 carbon, silica and silica activated carbon composite. Energy Procedia 50, 113–120.
458 https://doi.org/10.1016/j.egypro.2014.06.014.
459 Kleib, J., Aouad, G., Louis, G., Zakhour, M., Boulos, M., Rousselet, A., Bulteel, D., 2018. The
460 use of calcium sulfoaluminate cement to mitigate the alkali silica reaction in mortars. Constr.
461 Build. Mater. 184, 295–303. https://doi.org/10.1016/j.conbuildmat.2018.06.215.
462 Li, J., Zhen B.H., He, Y., Zhou, Y., Chen, X., Ruan, S., Yang, Y., Dai, C., Tang, L., 2018.
463 Antimony contamination, consequences and removal techniques. Ecotoxicol. Environ. Safe.
464 156, 125–134. https://doi.org/10.1016/j.ecoenv.2018.03.024.
465 Mlayah, A., Jellali, S., 2015. Study of continuous lead removal from aqueous solutions by
466 marble wastes: efficiencies and mechanisms. Int. J. Environ. Sci. Technol. 12, 2965–2978.
467 https://doi.org/10.1007/s13762-014-0715-8.
468 McBride, M.C., 1980. Chemisorption of Cd^{2+} on calcite surface. Soil Sci. Am. J. 44, 26–28.
469 Minceva, M., Fajgar, R., Markowska, I., Meshko, V., 2008. Comparative study of Zn^{2+}, Cd^{2+},
470 and Pb^{2+} removal from water solution using natural clinoptilolitic zeolite and commercial

granulated activated carbon. Equilibrium of adsorption. Sep. Sci. Technol. 43, 1–27. https://doi.org/10.1080/01496390801941174.

Okeola, F.O., Odebunmi, E.O., Nwosu, F.O., Abu, T.O., Mohammed, A.A., Samuel A.O., 2017. Removal of lead and cadmium ions from aqueous solution by adsorption onto *Jatrophas curcas* Activated Carbon. Nig. J. Pure Appl. Sci. 30, 2955–2964. https://doi.org/10.19240/njpas.2016.A30.

Pehlivan, E., Özkan, A.M., Dinç, S., Parlayici, S., 2009. Adsorption of Cu^{2+} and Pb^{2+} ion on dolomite powder. J. Hazard. Mater. 167, 1044–1049. https://doi.org/10.1016/j.jhazmat.2009.01.096.

Ponomarev, N., Pastushok, O., Repo, E., Doshi, B., Sillanpää, M., 2019. Lignin-Based Magnesium Hydroxide Nanocomposite. Synthesis and Application for the Removal of Potentially Toxic Metals from Aqueous Solution. ACS Appl. Nano Mater. 2, 5492–5503. https://doi.org/10.1021/acsanm.9b01083.

Qasem, N.A.A., Mohemmed, R.H., Lawal, D.U. 2021. Removal of heavy metal ions from wastewater: a comprehensive and critical review. *npj* Clean Water 4, 36. https://doi.org/10.1038/s41545-021-00127-0.

Rangel-Porras, G., García-Magno, J.B., Gonzáles-Munoz, M.P., 2010. Lead and cadmium immobilization on calcitic limestone materials. Desalination 262, 1–10. https://doi.org/10.1016/j.desal.2010.04.043.

Renu, Agarwal, M., Singh, K. 2017. Heavy metal removal from wastewater using various adsorbents: a review. J. Water Reuse Desalin. 7, 387–419. https://doi:10.2166/wrd.2016.104.

Santhosh, C., Malathi, A., Dhaneshvar, E., Bhatnagar, A., Grace, A.N., Madhavan, J., 2019. Iron oxide nanomaterials for water purification. Nanoscale Materials in Water Purification, 439–446. https://doi.org/10.1016/B978-0-12-813926-4.00022-7.

Sari, A., Mendil, D., Tuzen, M., Soylak, M., 2008. Biosorption of Cd(II) and Cr(III) from aqueous solution by moss (Hylocomium spendens) biomass: Equilibrium, kinetic and thermodynamic studies. Chem. Eng. J. 144, 1–9. https://doi.org/10.1016/j.cej.2007.12.020.

Savio, M., Cerutti, S., Martinez, L.D., Smichowski, P., Gil, R.A., 2010. Study of matrix and spectral interferences in the determination of lead in sediments, sludges and soils by SR-ETAAS using slurry sampling. Talanta 82, 523–527. https://doi.org/10.1016/j.talanta.2010.05.017.

Sturchio, N.C., Chiarello, R.P., Cheng, L., Lyman, P.F., Bedzyk, M.J., Qian, Y., You, H., Yee, D., Geissbuhler, P., Sorensen, L.B., Liang, Y., Baer, D.R., 1997. Lead adsorption at the calcite-water interface: synchrotron X-ray standingwave and X-ray reflectivity studies. Geochim. Cosmochim. Acta 61, 251–263. https://doi.org/10.1016/S0016-7037(96)00326-2.

Tariq, X., Saifullah, M., Anjum, T., Javed, M., Tayyrab, N., Shoukat, I., 2018. Removal of heavy metal from chemical industrial wastewater using agro based bio-sorbents. ACMY. 2, 9–14. https://doi.org/10.26480/acmy.02.2018.09.14.

Trivedi, P., Axe, L., Dyer, J., 2001. Adsorption of metal ions onto goethite: single adsorbate and competitive systems. Colloid. Surface A. 191, 107–121. https://doi.org/10.1016/S0927-7757(01)00768-3.

Thouvenin, B., Gonzales, J.L., Chiffoleau, J.F., Boutier, B., Le Hir, P., 2007. Modelling Pb and Cd dynamics in the Seine esturary. Hydrobiologia 588, 109–124. https://doi.org/10.1007/s10750-007-0656-z.

Ugwu, I.M., Igbokwe, O.A., 2019. Sorption of heavy metals on clay minerals and oxides: A review. Advanced Sorption Process Applications 1–24. https://doi.org/10.5772/intechopen.80989.

518 Wang, P., Shen, T., Li, X., Tang, Y., Li, Y., 2020. Magnetic Mesoporous Calcium Carbonate-
519 Based Nanocomposites for the Removal of Toxic Pb(II) and Cd(II) Ions from Water. ACS
520 Appl. Nano Mater. 3, 1272–1281. https://doi.org/10.1021/acsanm.9b02036.
521 Waterlot, C., Bidar, G., Pruvot, C., Douay F., 2011. Analysis of cadmium in water extracts from
522 contaminated soils with high arsenic and iron concentration levels. J. Environ. Sci. Eng. 5, 271–
523 280.
524 Waterlot, C., Douay, F., 2009. The problem of arsenic interference in the analysis of Cd to
525 evaluate its extractability in soils contaminated by arsenic. Talanta 80, 716–722.
526 https://doi.org/10.1016/j.talanta.2009.07.053.
527 Waterlot, C., Hechelski, M., 2019. Benefits of ryegrass on multicontaminated soils. Part 1:
528 Effects of fertilizers on bioavailability and accumulation of metals. Sustainability 11, 5093–
529 6013. https://doi.org/10.3390/su11185093.
530 Wolowiec, M., Komorowska-Kaufman, M., Pruss, A., Rsepa, G., Bajda, T., 2019. Removal of
531 heavy metals and metalloids from water using drinking water treatment residuals as adsorbents:
532 A review. Minerals 9, 487–504. https://doi.org/10.3390/min9080487.
533 Xu, P., Zeng, G.M., Huang, D.L., Feng, C.L., Hu, S., Zhao, M.H., Lai, C., Wei, Z., Huang, C.,
534 Xie, G.X., Liu, Z.F., 2012. Use of iron oxide nanomaterials in wastewater treatment: A review.
535 Sci. Total Environ. 424, 1–10. https://doi.org/10.1016/j.scitotenv.2012.02.023.
536 Yaqoob, A.A., Parveen, T., Umar, K., Ibrahim, M.N.M., 2020. Role of nanomaterials in the
537 treatment of wastewater: A review. Water 12, 495–525. https://doi.org/10.3390/w12020495.
538 Zaimee, M.Z.A., Sarjadi, M.S., Rahman, Md.L. 2021. Heavy metals removal from water by
539 efficient adsorbents. Water 13, 2659. https://doi.org/10.3390/w13192659.

Table 1. Main chemical composition of industrial wastes used as sorbents

	Ca (%)	Mg (%)	K (g kg^{-1})	Na (g kg^{-1})	Al (g kg^{-1})	Fe (g kg^{-1})	Mn (g kg^{-1})	Cd (mg kg^{-1})	Pb (mg kg^{-1})	Zn (mg kg^{-1})	Cu (mg kg^{-1})	As (mg kg^{-1})
IW1	22	5.5	1.8	0.3	6.87	6.4	0.8	0.2	3	42	1.5	7
IW2	5.8	21	0.65	0.7	0.65	0.65	0.02	0.5	0.8	5	1.1	0.5

Table 2. Results of the ANCOVA investigating the effects of the contaminant concentration in solutions, the filter types (CA, IW1 or IW2) and their interaction on the filtration of Cd and Pb.

Parameters	Df	Mean sq	Fvalue	*p*-value
Cd				
Initial concentration	1	432.2	228	10^{-16} ***
Sorbent	2	18.8	9.5	10^{-4} ***
Initial concentration × Sorbent	2	2.9	1.5	0.2
Residuals	165	1.9		
Pb				
Initial concentration	1	571.5	276.1	10^{-16} ***
Sorbent	2	38.2	18.4	10^{-7} ***
Initial concentration × Sorbent	2	0.5	0.3	0.8
Residuals	165	2.1		

Significance levels: '***' 0.001'**' 0.01'*' 0.05. Df: Degree of freedom, F-value: Fisher value, Mean sq: Mean of squares

Table 3. Results of the post-hoc Tukey analysis investigating the differences between ANCOVA models.

Parameters	Estimate	Std. Error	t-value	*p*-value
Cd				
IW1 - CA	-1.3590	0.3125	-4.344	10^{-4} ***
IW2 - CA	-1.3705	0.3125	-4.384	10^{-4} ***
IW2 - IW1	-0.0125	0.3125	-0.040	0.999
Pb				
IW1 - CA	-1.1370	0.2992	-3.800	10^{-4} ***
IW2 - CA	-1.1193	0.2992	-3.741	10^{-4} ***
IW2 - IW1	0.0177	0.2992	0.059	0.998

Significance levels: '***' 0.001'**' 0.01'*' 0.05. t-value: Student value, Std. Error : Standard error

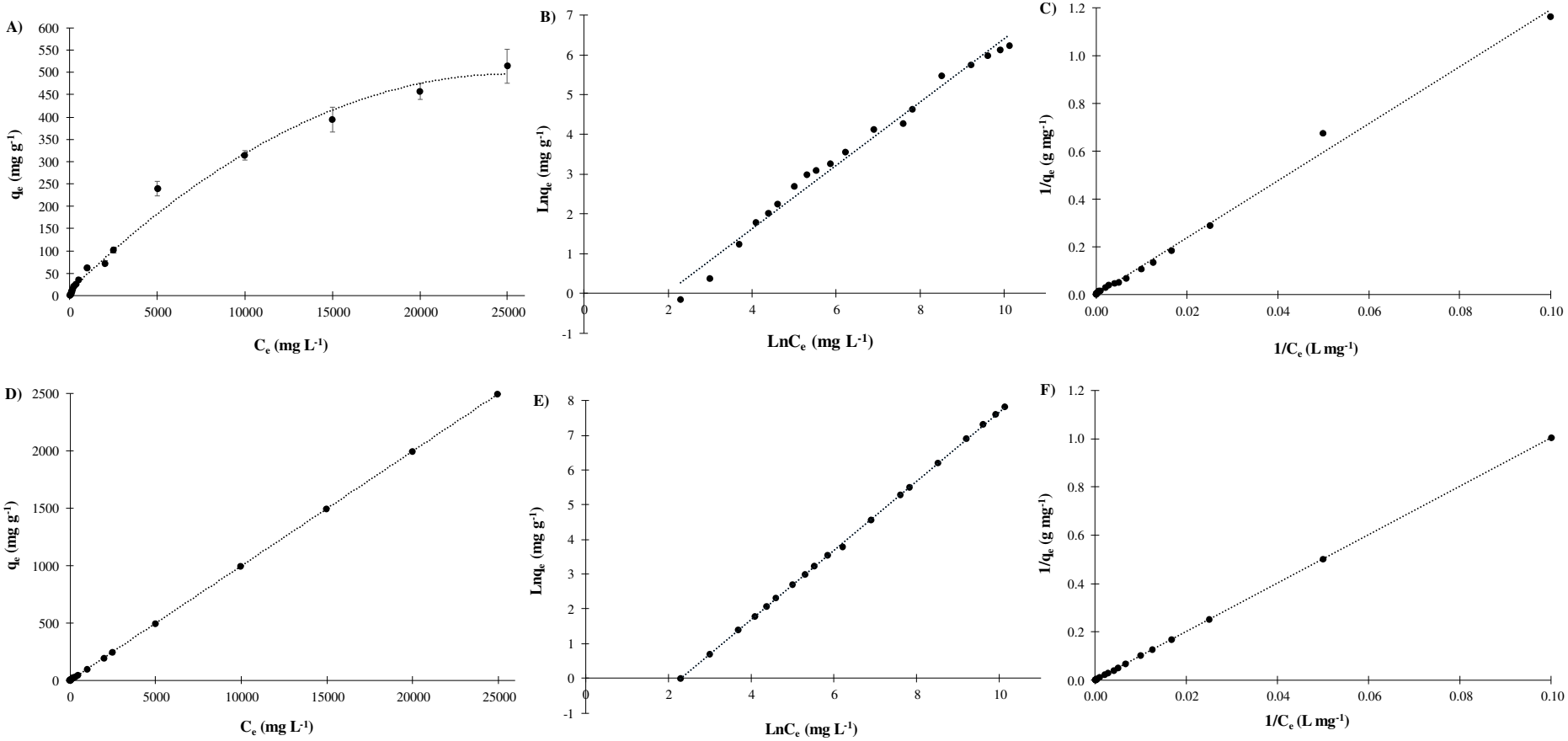

Figure 1: Freundlich and Langmuir isotherms of Cd (A, B, C) and Pb (D, E, F) on activated carbon (AC)

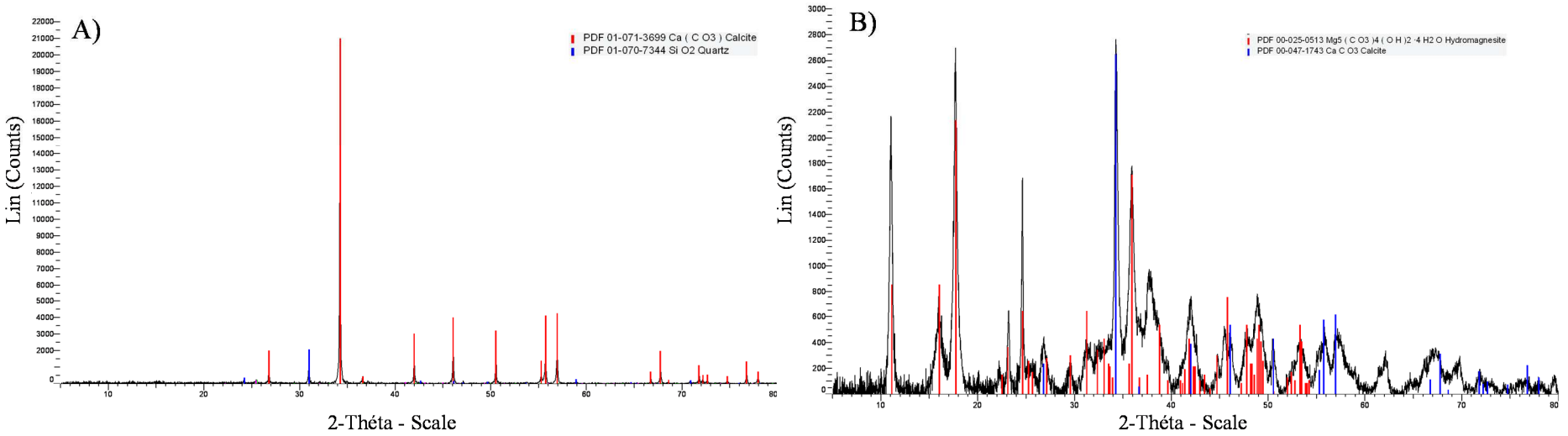

Figure 2: Characterization of IW1 (A) and IW2 (B) by XRD

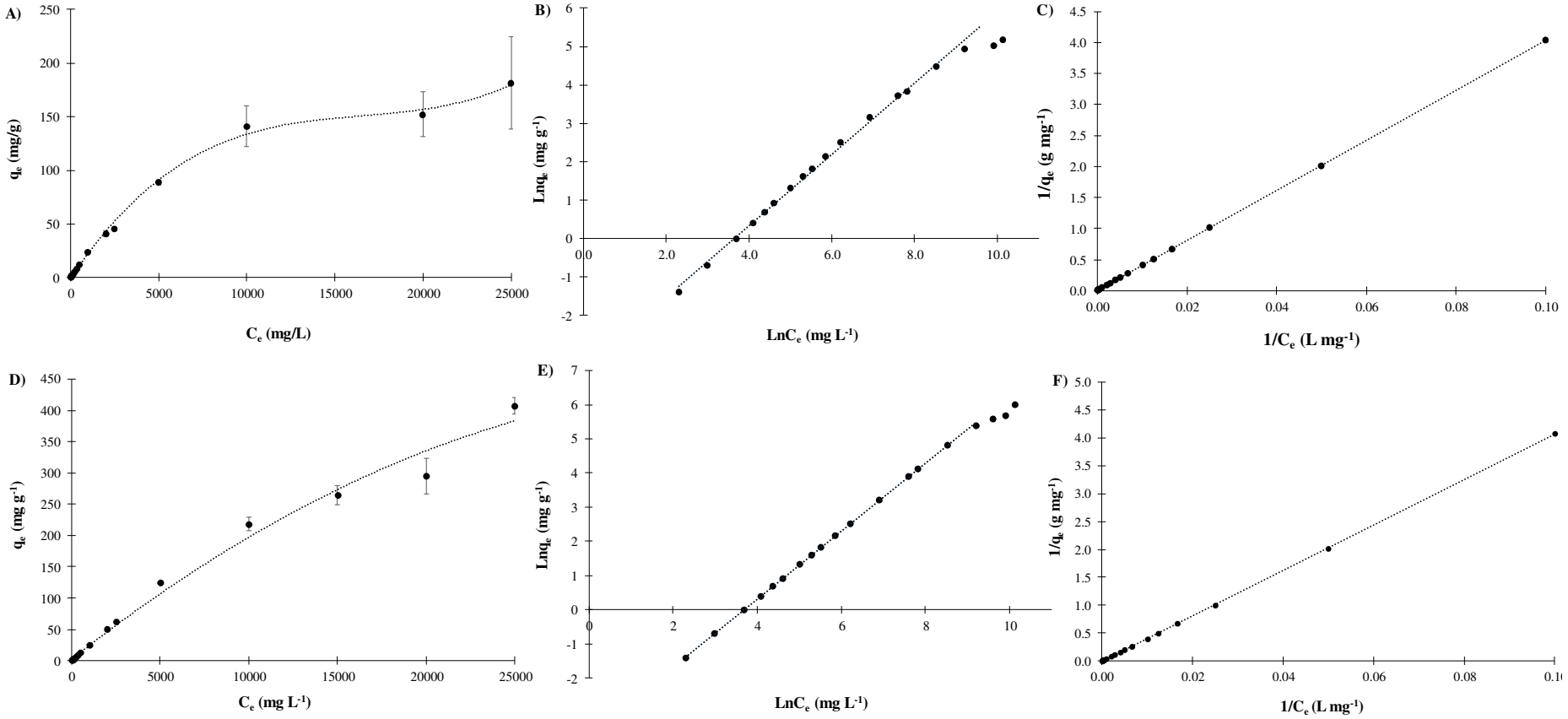

Figure 3: Freundlich and Langmuir isotherms of Cd (A, B, C) and Pb (D, E, F) on industrial waste IW1

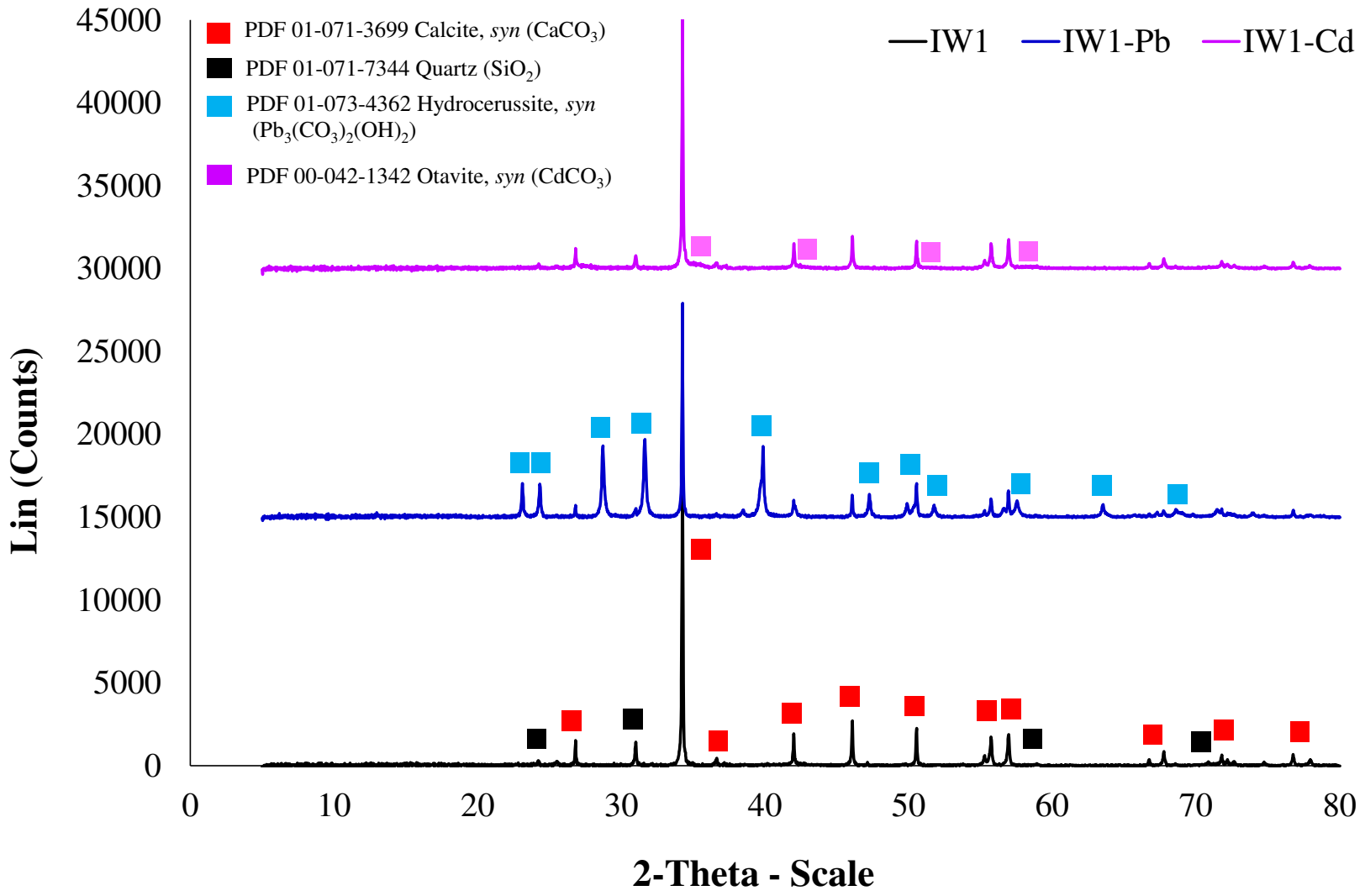

Figure 4: XRD diffraction pattern of IW1 before and after filtration (IW1-Cd, IW1-Pb)

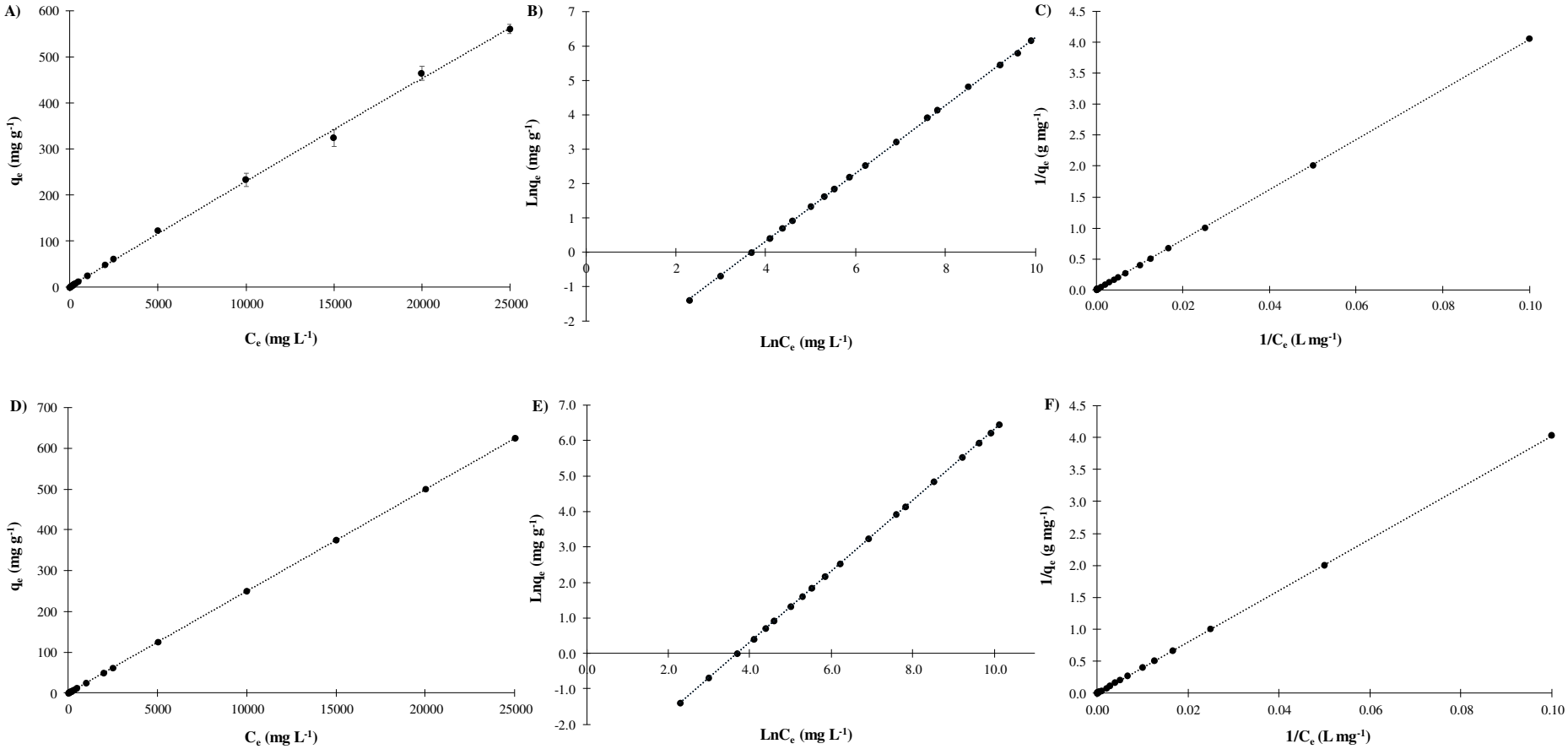

Figure 5: Freundlich and Langmuir isotherms of Cd (A, B, C) and Pb (D, E, F) on industrial waste IW2

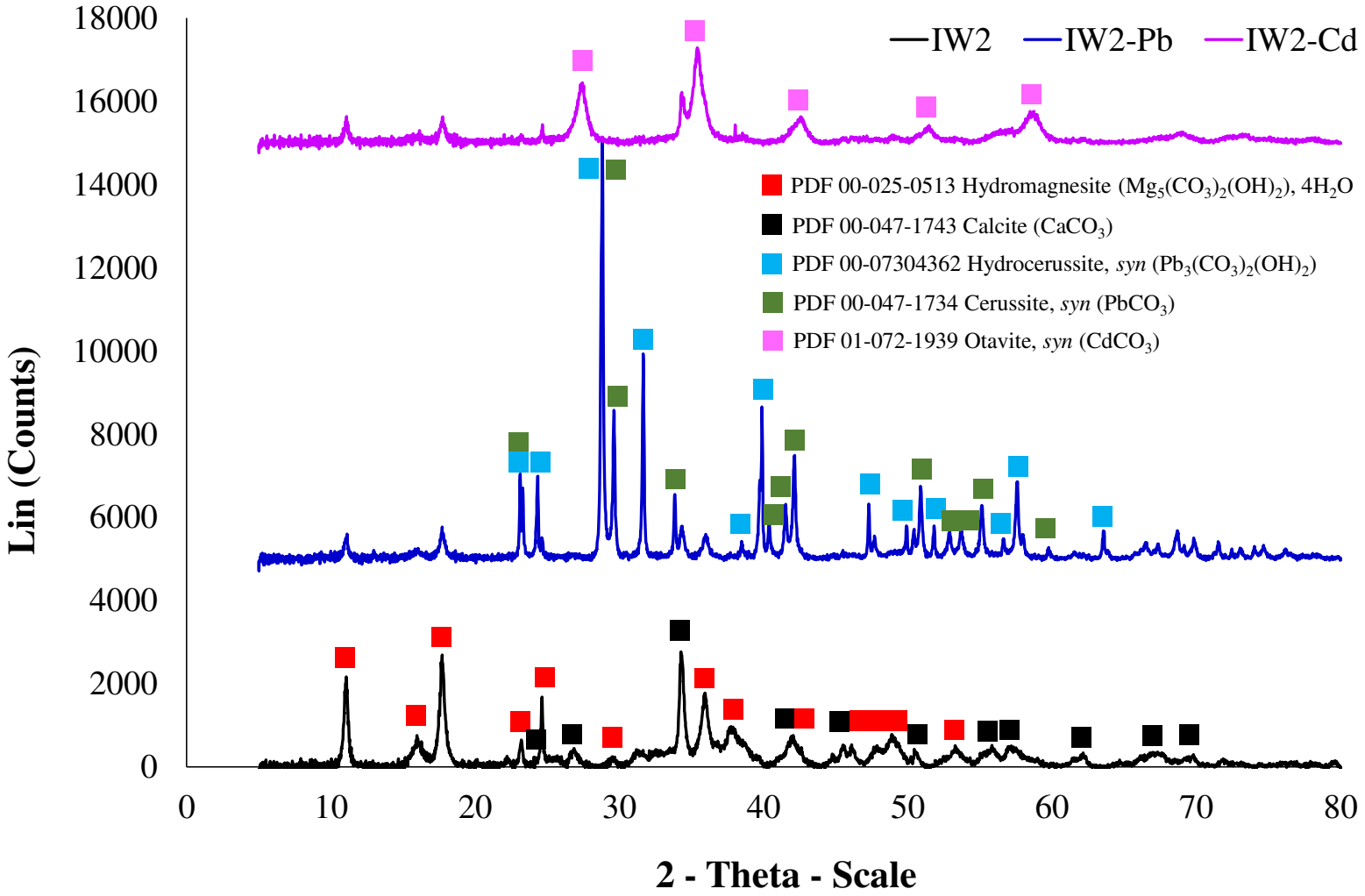

Figure 6: XRD diffraction pattern of IW2 before and after filtration (IW2-Cd, IW2-Pb)

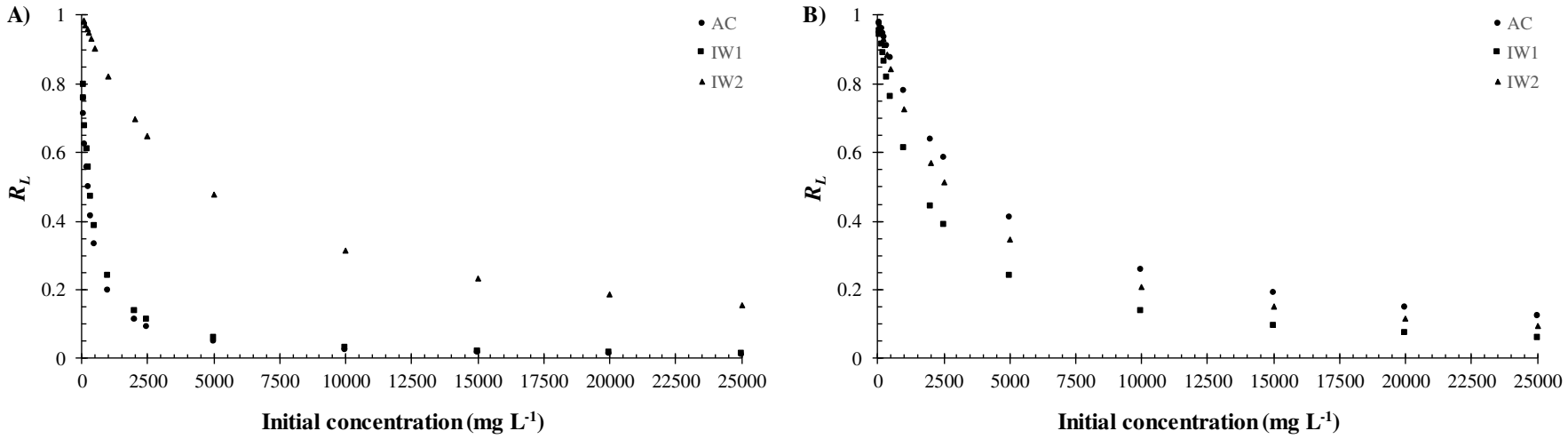

Figure 7: Variation of the Hall parameter: A) Cd and B) Pb

Contaminated water

2 studied pollutants

Cd=cadmium
Pb=lead

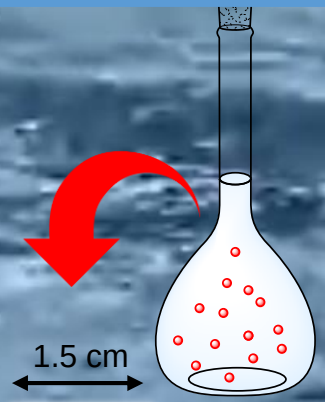

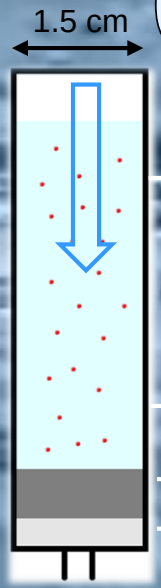

Contaminated water

Redisep Rf column

Sorbent

Cotton

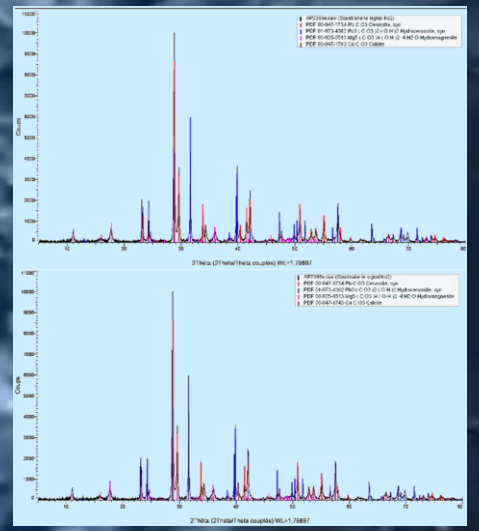

2 investigated sorbents

IW1=Industrial waste 1
IW2=Industrial waste 2

1 reference sorbent

AC=activated charcoal

Decontaminated water